

Study of the nonleptonic decay $\Xi_c^0 \rightarrow \Lambda_c^+ \pi^-$ in the covariant confined quark model

Mikhail A. Ivanov,¹ Valery E. Lyubovitskij,^{2,3,4} and Zhomart Tyulemissov^{1,5,6}

¹*Bogoliubov Laboratory of Theoretical Physics,
Joint Institute for Nuclear Research, 141980 Dubna, Russia*

²*Institut für Theoretische Physik, Universität Tübingen,
Kepler Center for Astro and Particle Physics,
Auf der Morgenstelle 14, D-72076 Tübingen, Germany*

³*Departamento de Física y Centro Científico Tecnológico de Valparaíso-CCTVal,
Universidad Técnica Federico Santa María, Casilla 110-V, Valparaíso, Chile*

⁴*Millennium Institute for Subatomic Physics at
the High-Energy Frontier (SAPHIR) of ANID,
Fernández Concha 700, Santiago, Chile*

⁵*The Institute of Nuclear Physics,
Ministry of Energy of the Republic of Kazakhstan, 050032 Almaty, Kazakhstan*

⁶*Al-Farabi Kazakh National University, 050040 Almaty, Kazakhstan*

Abstract

The nonleptonic decay $\Xi_c^0 \rightarrow \Lambda_c^+ \pi^-$ with $\Delta C = 0$ is systematically studied in the framework of the covariant confined quark model accounting for both short and long distance effects. The short distance effects are induced by four topologies of external and internal weak W^\pm exchange, while long distance effects are saturated by an inclusion of the so-called pole diagrams with an intermediate $\frac{1}{2}^+$ and $\frac{1}{2}^-$ baryon resonances. The contributions from $\frac{1}{2}^+$ resonances are calculated straightforwardly by accounting for single charmed Σ_c^0 and $\Xi_c'^+$ baryons whereas the contributions from $\frac{1}{2}^-$ resonances are calculated by using the well-known soft-pion theorem in the current-algebra approach. It allows to express the parity-violating S-wave amplitude in terms of parity-conserving matrix elements. It is found that the contribution of external and internal W -exchange diagrams is significantly suppressed by more than one order of magnitude in comparison with data. The pole diagrams play the major role to get consistency with experiment.

I. INTRODUCTION

The study of the heavy-flavor-conserving nonleptonic weak decays of heavy baryons has received a lot of attention due to their observation and measurement of branching fractions by the LHCb and Belle collaborations. The decay $\Xi_c^0 \rightarrow \Lambda_c^+ + \pi^-$ was first observed at LHCb experiment and the branching fraction was measured to be $\mathcal{B} = (0.55 \pm 0.02 \pm 0.18)\%$ [1]. Recent experimental data obtained by the Belle collaboration gave the value of $\mathcal{B}(\Xi_c^0 \rightarrow \Lambda_c^+ + \pi^-) = (0.54 \pm 0.05 \pm 0.12)\%$ [2] which is in perfect agreement with the LHCb result.

The recent theoretical review of nonleptonic two-body decays of single and doubly charm baryons was given in Ref. [3]. The review was aiming to shed new light on the standard current algebra approach to such processes.

The heavy-flavor-conserving nonleptonic weak decays of heavy baryons were studied in [4] in the formalism which incorporates both the heavy quark symmetry and the chiral symmetry. The branching fractions of specific nonleptonic decays such as $\Xi_c \rightarrow \Lambda_c^+ \pi$ are found to be of the order of 10^{-4} .

The weak decays $\Xi_b \rightarrow \Lambda_b \pi$ and $\Xi_c \rightarrow \Lambda_c^+ \pi$, in which the heavy quark is not destroyed, have been discussed in Ref. [5]. It was shown that these should go at the rate of order $\approx 0.01 \text{ ps}^{-1}$. In the updated research [6] of the Voloshin's approach, the new measurements by LHCb [7] of the lifetimes of the Λ_c^+ , Ξ_c^+ and Ξ_c^0 charm baryons have been used to predict a lower bound on the rate of the decays $\Xi_c^0 \rightarrow \Lambda_c^+ \pi$. It was found that $\mathcal{B}(\Xi_c^0 \rightarrow \Lambda_c^+ + \pi^-) > \mathcal{B}_{\min} = (0.25 \pm 0.15) \times 10^{-3}$.

The heavy flavor conserving decays of strange charmed baryons proceed via two subprocesses, first, via decay $s \rightarrow u(\bar{u}d)$ (or equivalently, via the transition $us \rightarrow ud$), and, second, via the transition $cs \rightarrow cd$. In Ref. [8] it was shown that a second term is approximately equal to the first term. But it was unclear whether they interfere destructively or constructively. For constructive interference it was found that $\mathcal{B}(\Xi_c^0 \rightarrow \Lambda_c^+ + \pi^-) = (1.94 \pm 0.70) \times 10^{-3}$. For destructive interference, the value of branching fraction is expected to be less than about 10^{-4} .

In Ref. [9] the upper bound for the decay width $\Gamma(\Xi_c^0 \rightarrow \Lambda_c^+ + \pi^-) < 1.7 \times 10^{-14} \text{ GeV}$ was obtained by using the Voloshin's approach. In work [10] the four-quark matrix element of heavy-flavor-conserving hadronic weak decays was evaluated in using two different models: the MIT bag model and the diquark model. All calculations included only S-wave amplitudes

and obtained $\mathcal{B}(\Xi_c^0 \rightarrow \Lambda_c^+ + \pi^-) = 1.7 \times 10^{-7}$ for MIT bag model and $\mathcal{B}(\Xi_c^0 \rightarrow \Lambda_c^+ + \pi^-) = 0.87 \times 10^{-4}$ for diquark model. In updated work [11] it was confirmed that $\Xi_c \rightarrow \Lambda_c^+ \pi$ decays are indeed dominated by the parity-conserving transition induced from nonspectator W -exchange and that they receive largest contributions from the intermediate Σ_c^0 pole terms. Also they obtained that the asymmetry parameter α is positive, of order $0.70_{-0.17}^{+0.13}$ and $\mathcal{B}(\Xi_c^0 \rightarrow \Lambda_c^+ + \pi^-) = 1.76_{-0.12}^{+0.18} \times 10^{-3}$. In [12] the wave functions from the homogeneous bag model are adopted in order to remove the center-of-mass motion of the static bag. The calculations have been carried out under the same framework, and it has been shown that the matrix elements of four-quark operators are enhanced about twice and for $\mathcal{B}(\Xi_c^0 \rightarrow \Lambda_c^+ + \pi^-) = (7.2 \pm 0.7) \times 10^{-3}$.

It was investigated pion emission and pole terms in the heavy quark conserving weak decay of Ξ_c^0 in the framework of non-relativistic constituent quark model [13]. The parity-conserving pole terms are found dominant and the direct pion emission contributions are rather small and $\mathcal{B}(\Xi_c^0 \rightarrow \Lambda_c^+ + \pi^-) = (0.58 \pm 0.21)\%$ with uncertainties caused by the quark model parameters with 20% errors.

This work is aiming to study the decay $\Xi_c^0 \rightarrow \Lambda_c^+ + \pi^-$ in the framework of the covariant confined quark model (CCQM) previously developed by us, see Ref. [14]. This approach found many applications, particularly, in physics of heavy baryons, see Refs. [15–32]. One of the important step in development of the CCQM was done in Ref. [15] where *ab initio* three-loop quark model calculation of the W -exchange contribution to the nonleptonic two-body decays of the doubly charmed baryons Ξ_{cc}^{++} and Ω_{cc}^+ have been made. The W -exchange contributions appear in addition to the factorizable contributions and, generally, are not suppressed. In [16] such an approach was extended to study two-body nonleptonic decays of light lambda hyperon $\Lambda \rightarrow p\pi^-(n\pi^0)$ with account for both short and long distance effects. It was shown that the contribution from the W -exchange diagrams is sizably suppressed and basically the pole diagrams allow to describe the experimental data for the branching fractions.

The paper is organized as follows. In Sec. II we briefly discuss the classification and spectroscopy of singly charmed $1/2^+$ baryons. Then we give the basic ingredients and milestones that are needed for calculation of two-body nonleptonic decays including both the W -exchange quark and pole diagrams. Sec. III is devoted to calculation of the matrix elements and branching fraction of the decay $\Xi_c^0 \rightarrow \Lambda_c^+ + \pi^-$. We discuss in details the

classification of the diagrams appearing in these decays and give the analytical expressions for matrix elements. In Sec. IV we present numerical results for the amplitudes and branching fractions. We compare them with those available in the literature. Finally, in Sec. V we make conclusions and summarize the main results obtained in this paper.

II. THE SINGLY CHARMED BARYONS

The masses of singly charmed baryons have been predicted in one gluon exchange model developed in Ref. [33]. The comprehensive review on heavy baryons, their spectroscopy, semileptonic and nonleptonic decays may be found in Ref. [34]. In Tables I we display the names, quark contents and interpolating currents of the low-lying multiplets of singly charmed baryons with spin 1/2. For singly charmed baryons the flavor decomposition of the diquark, made of (u, d, s) -quarks is $3 \otimes 3 = \bar{3}_A + 6_S$ (A=antisymmetric, S=symmetric). The values of masses with errors are taken from particle data group (PDG) [35].

TABLE I: Singly charmed $1/2^+$ baryon states. Notation $[a, b]$ and $\{a, b\}$ for antisymmetric and symmetric flavor index combinations.

Title	Content	$SU(3)$	(I, I_3)	Current	Mass (MeV)
Λ_c^+	$c[ud]$	$\bar{3}$	(0,0)	$\epsilon^{abc}c^a(u^b C \gamma_5 d^c)$	2286.46 ± 0.14
Ξ_c^+	$c[us]$	$\bar{3}$	(1/2,1/2)	$\epsilon^{abc}c^a(u^b C \gamma_5 s^c)$	2467.71 ± 0.23
Ξ_c^0	$c[ds]$	$\bar{3}$	(1/2,-1/2)	$\epsilon^{abc}c^a(d^b C \gamma_5 s^c)$	2470.44 ± 0.28
Σ_c^{++}	cuu	6	(1,1)	$\epsilon^{abc}\gamma_\mu\gamma_5c^a(u^b C \gamma^\mu u^c)$	2453.97 ± 0.14
Σ_c^+	$c\{ud\}$	6	(1,0)	$\epsilon^{abc}\gamma_\mu\gamma_5c^a(u^b C \gamma^\mu d^c)$	2452.65 ± 0.22
Σ_c^0	cdd	6	(1,-1)	$\epsilon^{abc}\gamma_\mu\gamma_5c^a(d^b C \gamma^\mu d^c)$	2453.75 ± 0.14
$\Xi_c^{\prime+}$	$c\{us\}$	6	(1/2,1/2)	$\epsilon^{abc}\gamma_\mu\gamma_5c^a(u^b C \gamma^\mu s^c)$	2578.2 ± 0.5
$\Xi_c^{\prime0}$	$c\{ds\}$	6	(1/2,-1/2)	$\epsilon^{abc}\gamma_\mu\gamma_5c^a(d^b C \gamma^\mu s^c)$	2578.7 ± 0.5
Ω_c^0	css	6	(0,0)	$\epsilon^{abc}\gamma_\mu\gamma_5c^a(s^b C \gamma^\mu s^c)$	2695.2 ± 1.7

We are aiming to study the two-body nonleptonic decay $\Xi_c^0 \rightarrow \Lambda_c^+ \pi^-$ which branching fraction was measured for the first time by LHCb collaboration [1]. The effective Hamiltonian

relevant for this purpose is written as

$$\mathcal{H}_{\text{eff}}^{\Delta S=1} = \frac{G_F}{\sqrt{2}} \left[V_{us}^* V_{ud} \left(C_1^{(u)}(\mu_u) Q_1^{(u)} + C_2^{(u)}(\mu_u) Q_2^{(u)} \right) + V_{cs}^* V_{cd} \left(C_1^{(c)}(\mu_c) Q_1^{(c)} + C_2^{(c)}(\mu_c) Q_2^{(c)} \right) + \text{H.c.} \right] \quad (1)$$

where Q_1 and Q_2 is the set of flavor-changing effective four-quark operators given by

$$\begin{aligned} Q_1^{(u)} &= (\bar{s}_a O_L^\mu u_b)(\bar{u}_b O_{\mu L} d_a), & Q_2^{(u)} &= (\bar{s}_a O_L^\mu u_a)(\bar{u}_b O_{\mu L} d_b), \\ Q_1^{(c)} &= (\bar{s}_a O_L^\mu c_b)(\bar{c}_b O_{\mu L} d_a), & Q_2^{(c)} &= (\bar{s}_a O_L^\mu c_a)(\bar{c}_b O_{\mu L} d_b). \end{aligned} \quad (2)$$

Here $O_L^\mu = \gamma^\mu(1 - \gamma_5)$ is the left-handed chiral weak matrix. One has to note that we adopt the numeration of the operators from Ref. [36] where the $C_2 Q_2$ means the leading order whereas the $C_1 Q_1$ is for subleading order. The numerical values of the Wilson coefficients C_1 and C_2 from Ref. [36] are being equal to

$$\begin{aligned} C_1^{(u)}(\mu_u) &= -0.625, & C_2^{(u)}(\mu_u) &= 1.361, & (\mu_u &= O(1 \text{ GeV})), \\ C_1^{(c)}(\mu_c) &= -0.621, & C_2^{(c)}(\mu_c) &= 1.336, & (\mu_c &= O(m_c)). \end{aligned} \quad (3)$$

We do not include penguin operators because their Wilson coefficients are small compare with those from current-current operators.

In the standard model (SM) the relation $V_{cs}^* V_{cd} = -V_{us}^* V_{ud}$ holds to an excellent approximation. For instance, in the Wolfenstein parametrization of the Cabibbo-Kobayashi-Maskawa (CKM) matrix, one has $V_{us}^* V_{ud} = +\lambda(1 - \lambda^2) + O(\lambda^4)$ whereas $V_{cs}^* V_{cd} = -\lambda(1 - \lambda^2) + O(\lambda^4)$. The global fit in the SM for the Wolfenstein parameter gives $\lambda = 0.22500 \pm 0.00067$. In what follows, we introduce the short notations

$$V_{\text{CKM}}^{(u)} = |V_{us}^* V_{ud}|, \quad \text{and} \quad V_{\text{CKM}}^{(c)} = -|V_{cs}^* V_{cd}|. \quad (4)$$

The numerical values of the CKM matrix elements needed in our calculations are taken from PDG [35]:

$$\begin{aligned} |V_{ud}| &= 0.97373 \pm 0.00031, & |V_{us}| &= 0.2243 \pm 0.0008, \\ |V_{cd}| &= 0.221 \pm 0.004, & |V_{cs}| &= 0.975 \pm 0.006, \end{aligned} \quad (5)$$

that approximately give $V_{\text{CKM}}^{(u)} \approx 0.218$ and $V_{\text{CKM}}^{(c)} \approx -0.215$.

The quark diagrams that contribute to the Cabibbo-favored decay are shown in Fig. 1. After hadronization, the diagram Ia factorizes out into two parts: the weak transition $\Xi_c^0 \rightarrow \Lambda_c^+$ via the W -emission and the matrix element describing the pion leptonic decay. The W -exchange diagrams IIa, IIb and III contribute into both the pure quark diagrams called the short distance (SD) contributions and effectively into the pole diagrams shown in Fig. 2. They describe the so-called long distance (LD) contributions. For instance, the diagrams IIa and III effectively generate the Σ_c^0 -resonance diagram, whereas the diagram IIb effectively generates the Ξ_c^+ and $\Xi_c'^+$ -resonance diagrams.

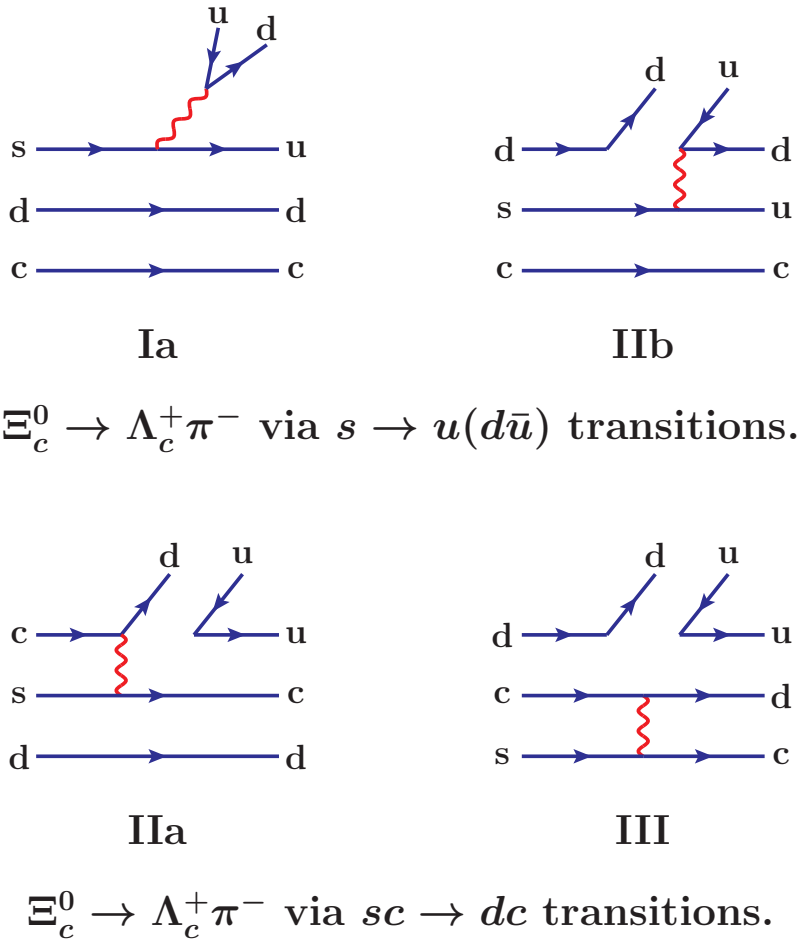


FIG. 1: Flavor-color topologies for $\Xi_c^0 \rightarrow \Lambda_c^+ \pi^-$ decay: Ia is the tree level diagram, IIa, IIb and III are the W -exchange diagrams.

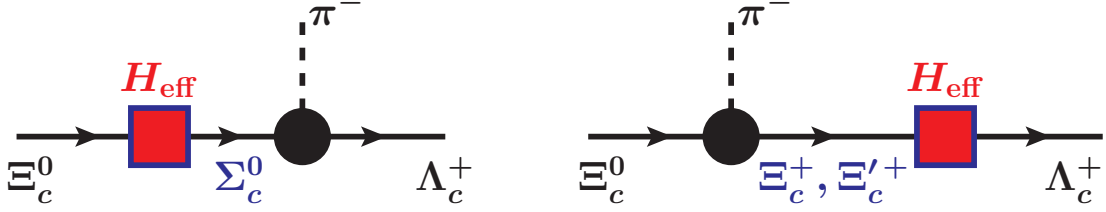


FIG. 2: The pole diagrams which effectively account for the long-distance contributions.

III. MATRIX ELEMENTS AND DECAY WIDTHS

We are going to calculate the matrix elements of nonleptonic decays of Ξ_c^0 -baryon in the framework of the CCQM developed in our previous papers. The starting point is the Lagrangian describing couplings of the baryon field with its interpolating quark current.

$$\mathcal{L}(x) = g_B \bar{B}(x) J(x) + \text{H.c.}, \quad (6)$$

where the coupling constant g_B is determined from the so-called *compositeness condition*, which was proposed by Salam and Weinberg [37, 38] and extensively used in the literature (see, e.g., Refs. [39, 40]).

The nonlocal extension of the interpolating currents shown in Table I reads

$$J_B(x) = \int dx_1 \int dx_2 \int dx_3 F_B(x; x_1, x_2, x_3) \varepsilon_{abc} \Gamma_1 q_1^a(x_1) (q_2^b(x_2) C \Gamma_2 q_3^c(x_3)),$$

$$F_B(x; x_1, x_2, x_3) = \delta^{(4)}\left(x - \sum_{i=1}^3 w_i x_i\right) \Phi_B\left(\sum_{i<j} (x_i - x_j)^2\right), \quad (7)$$

where $w_i = m_i / (\sum_{j=1}^3 m_j)$ and m_i is the mass of the quark at the space-time point x_i . The matrices Γ_1, Γ_2 are the Dirac strings of the initial and final baryon states as specified in Table I. The vertex function Φ_B is written as

$$\Phi_B\left(\sum_{i<j} (x_i - x_j)^2\right) = \int \frac{dq_1}{(2\pi)^4} \int \frac{dq_2}{(2\pi)^4} e^{-iq_1(x_1-x_3) - iq_2(x_2-x_3)} \tilde{\Phi}_B\left(-\vec{\Omega}_q^2\right),$$

$$\tilde{\Phi}_B\left(-\vec{\Omega}_q^2\right) = \exp\left(\vec{\Omega}_q^2 / \Lambda_B^2\right), \quad \vec{\Omega}_q^2 = \frac{1}{2}(q_1 + q_2)^2 + \frac{1}{6}(q_1 - q_2)^2 = \frac{2}{3} \sum_{i \leq j} q_i q_j. \quad (8)$$

For simplicity and calculational advantages we mostly adopted a Gaussian form for the functions $\tilde{\Phi}_B$. Here Λ_B is the size parameter for a given baryon. The size parameter phenomenologically describes the distribution of the constituent quarks in the given baryon.

In our approach the matrix elements contributing to the baryon transitions $\Xi_c^0 \rightarrow \Lambda_c^+ \pi^-$ are represented by a set of the quark diagrams shown in Fig. 3. They describe the so-called short distance contributions.

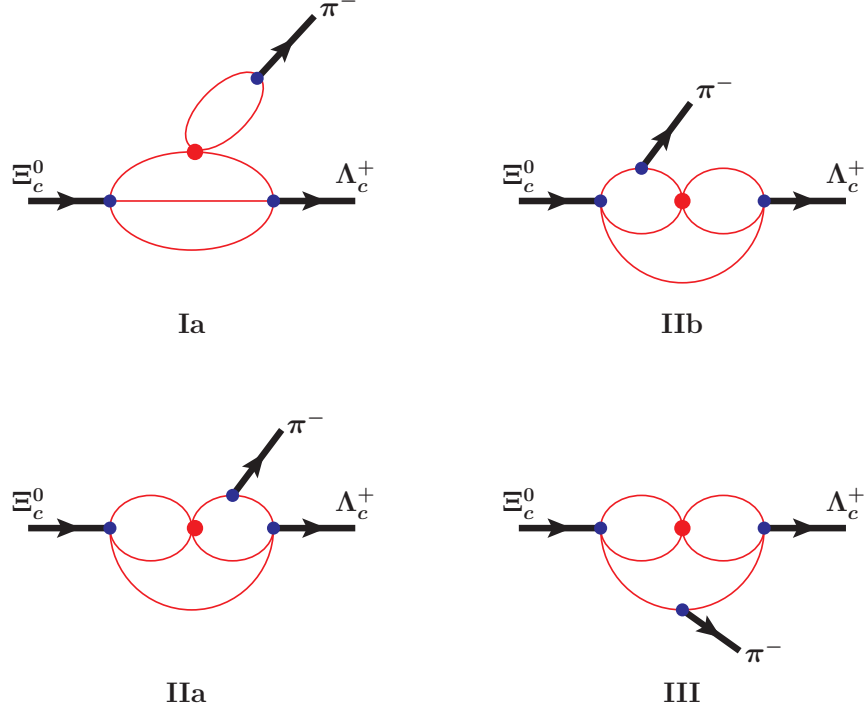


FIG. 3: Quark diagrams describing the SD-contributions

The diagrams describing the building blocks of the LD-contributions are shown in Fig. 4.

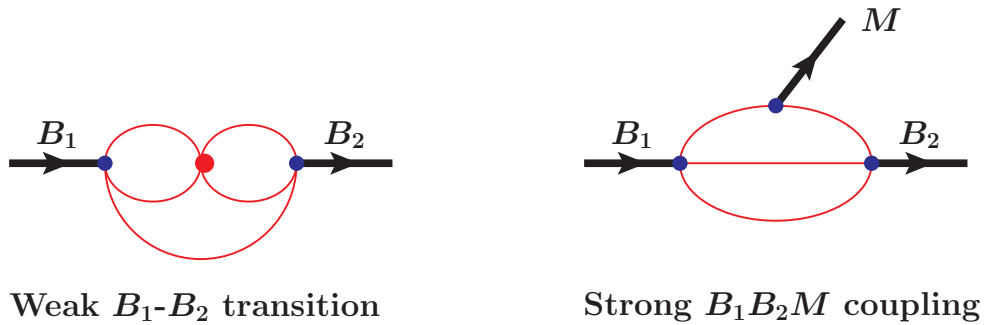


FIG. 4: Feynman diagrams describing the building blocks of the LD-contributions

First, we discuss the matrix elements corresponding to the SD-contributions. One has

$$M_{\text{SD}}(\Xi_c^0 \rightarrow \Lambda_c^+ \pi^-) = \frac{G_F}{\sqrt{2}} \left\{ V_{\text{CKM}}^{(u)} \bar{u}(p_2) \left[(C_2^{(u)} + \xi C_1^{(u)}) D_{\text{Ia}} + (C_2^{(u)} - C_1^{(u)}) D_{\text{IIb}} \right] u(p_1) \right. \\ \left. + V_{\text{CKM}}^{(c)} (C_2^{(c)} - C_1^{(c)}) \bar{u}(p_2) \left[D_{\text{IIa}} + D_{\text{III}} \right] u(p_1) \right\}. \quad (9)$$

Here, the factor $\xi = 1/N_c$ where N_c is the number of colors. This factor is set to zero in the numerical calculations according to the widely accepted phenomenology of the nonleptonic decays.

The contribution from the tree diagram factorizes into two pieces

$$D_{\text{Ia}} = N_c g_M \int \frac{d^4 k}{(2\pi)^{4i}} \tilde{\Phi}_M(-k^2) \text{tr} [O_L^\mu S_u(k - w_u q) \gamma_5 S_d(k + w_d q)] \\ \times 6 g_{B_1} g_{B_2} \int \frac{d^4 k_1}{(2\pi)^{4i}} \int \frac{d^4 k_2}{(2\pi)^{4i}} \tilde{\Phi}_{B_1}(-\vec{\Omega}_q^2) \tilde{\Phi}_{B_2}(-\vec{\Omega}_r^2) \\ \times S_c(k_2) \text{tr} [S_u(k_1 + p_2) O_{\mu L} S_s(k_1 + p_1) \gamma_5 S_d(k_1 + k_2) \gamma_5] \\ = -6 f_M q^\mu g_{B_1} g_{B_2} \int \frac{d^4 k_1}{(2\pi)^{4i}} \int \frac{d^4 k_2}{(2\pi)^{4i}} \tilde{\Phi}_{B_1}(-\vec{\Omega}_q^2) \tilde{\Phi}_{B_2}(-\vec{\Omega}_r^2) \\ \times S_c(k_2) \text{tr} [S_u(k_1 + p_2) O_{\mu L} S_s(k_1 + p_1) \gamma_5 S_d(k_1 + k_2) \gamma_5] \quad (10)$$

where $q_1 = k_2 - w_1^{\text{in}} p_1$, $q_2 = -k_1 - k_2 - w_2^{\text{in}} p_1$ and $r_1 = -k_2 + w_1^{\text{out}} p_2$, $r_2 = -k_1 - p_2 + w_2^{\text{out}} p_2$. The expression for $\vec{\Omega}^2$ is given by Eq. (8). Hereafter we adopt the brief notations B_1 for the ingoing baryon with the momentum p_1 , B_2 for the outgoing baryon with the momentum p_2 and M for the outgoing meson with the momentum q . The minus sign in front of f_M appears because the momentum q flows in the opposite direction from the decay of M -meson.

The calculation of the three-loop W -exchange diagrams is much more involved because the matrix element does not factorize. One has

$$D_{\text{IIb}} = 12 g_{B_1} g_{B_2} g_M \left[\prod_{i=1}^3 \int \frac{d^4 k_i}{(2\pi)^{4i}} \right] \tilde{\Phi}_{B_1}(-\vec{\Omega}_q^2) \tilde{\Phi}_{B_2}(-\vec{\Omega}_r^2) \tilde{\Phi}_M(-P^2) \\ \times S_c(k_3) \text{tr} [\gamma_5 S_d(k_2 + p_2) (1 + \gamma_5) S_u(k_2 + k_3)] \\ \times \text{tr} [S_u(k_1 + p_2) \gamma_5 S_d(k_1 + p_1) \gamma_5 S_s(k_1 + k_3) (1 - \gamma_5)], \\ q_1 = k_3 - w_1^{\text{in}} p_1, \quad q_2 = k_1 + p_1 - w_2^{\text{in}} p_1, \\ r_1 = -k_3 + w_1^{\text{out}} p_2, \quad r_2 = k_2 + k_3 + w_2^{\text{out}} p_2, \quad P = k_1 + w_u p_1 + w_d p_2. \quad (11)$$

$$\begin{aligned}
D_{\text{IIa}} &= 6g_{B_1}g_{B_2}g_M \left[\prod_{i=1}^3 \int \frac{d^4k_i}{(2\pi)^{4i}} \right] \tilde{\Phi}_{B_1} \left(-\vec{\Omega}_q^2 \right) \tilde{\Phi}_{B_2} \left(-\vec{\Omega}_r^2 \right) \tilde{\Phi}_M(-P^2) \\
&\times S_c(k_3 - k_2) O_L^\mu S_c(k_1 + p_1) \text{tr} [S_d(k_3) \gamma_5 S_u(k_2 + p_2) \gamma_5 S_d(k_2 + p_1) O_{\mu L} S_s(k_3 - k_1) \gamma_5] \\
q_1 &= k_1 + p_1 - w_1^{\text{in}} p_1, \quad q_2 = -k_3 - w_2^{\text{in}} p_1, \\
r_1 &= k_2 - k_3 + w_1^{\text{out}} p_2, \quad r_2 = -k_2 - p_2 + w_2^{\text{out}} p_2, \quad P = k_2 + w_u p_1 + w_d p_2. \quad (12)
\end{aligned}$$

$$\begin{aligned}
D_{\text{III}} &= 6g_{B_1}g_{B_2}g_M \left[\prod_{i=1}^3 \int \frac{d^4k_i}{(2\pi)^{4i}} \right] \tilde{\Phi}_{B_1} \left(-\vec{\Omega}_q^2 \right) \tilde{\Phi}_{B_2} \left(-\vec{\Omega}_r^2 \right) \tilde{\Phi}_M(-P^2) \\
&\times S_c(k_3) O_L^\mu S_c(k_2) \text{tr} [S_d(k_1 + k_3) \gamma_5 S_u(k_1 + p_2) \gamma_5 S_d(k_1 + p_1) \gamma_5 S_s(k_1 + k_2) O_{\mu R}] \\
q_1 &= k_2 - w_1^{\text{in}} p_1, \quad q_2 = k_1 + p_1 - w_2^{\text{in}} p_1, \\
r_1 &= -k_3 + w_1^{\text{out}} p_2, \quad r_2 = -k_1 - p_2 + w_2^{\text{out}} p_2, \quad P = k_1 + w_u p_1 + w_d p_2. \quad (13)
\end{aligned}$$

The calculation of the three-loop integrals proceeds in two steps, first, one has to perform the loop integration by using Fock-Schwinger representation for the quark propagators and Gaussian form for the vertex functions. This allows one to do tensor loop integrals in a very efficient way since one can convert loop momenta into derivatives of the exponent function. The calculations are done by using a FORM code which works for any numbers of loops and propagators. Second, one has to calculate the obtained integrals numerically over Fock-Schwinger variables by adopting the quark confinement ansatz. The numerical calculations are done by using the FORTRAN codes which include the output from the FORM code written in the format of double precision accuracy. Since the files with the output from FORM contain several thousand lines we are unable to show them in the paper. The details of such calculations may be found in our recent papers [22, 24]. The calculation is quite time consuming both analytically and numerically.

Finally, the matrix element describing the SD-contributions are written as

$$M_{\text{SD}}(\Xi_c^0 \rightarrow \Lambda_c^+ \pi^-) = \frac{G_F}{\sqrt{2}} \bar{u}(p_2) \left(A_{\text{SD}} + \gamma_5 B_{\text{SD}} \right) u(p_1), \quad (14)$$

where

$$\begin{aligned}
A_{\text{SD}} &= V_{\text{CKM}}^{(u)} \left[(C_2^{(u)} + \xi C_1^{(u)}) a_{\text{Ia}} + (C_2^{(u)} - C_1^{(u)}) a_{\text{IIb}} \right] + V_{\text{CKM}}^{(c)} (C_2^{(c)} - C_1^{(c)}) \left(a_{\text{IIa}} + a_{\text{III}} \right), \\
B_{\text{SD}} &= V_{\text{CKM}}^{(u)} \left[(C_2^{(u)} + \xi C_1^{(u)}) b_{\text{Ia}} + (C_2^{(u)} - C_1^{(u)}) b_{\text{IIb}} \right] + V_{\text{CKM}}^{(c)} (C_2^{(c)} - C_1^{(c)}) \left(b_{\text{IIa}} + b_{\text{III}} \right).
\end{aligned}$$

Now, we discuss the matrix elements corresponding to the LD contributions. The contribution coming from the pole diagram in Fig. 2 with the Σ_c^0 -resonance is written as

$$M_{\Sigma_c^0} = \frac{G_F}{\sqrt{2}} V_{\text{CKM}}^{(c)} \left(C_1^{(c)} - C_2^{(c)} \right) \bar{u}(p_2) D_{\Sigma_c^0 \Lambda_c^+ \pi^-}(p_1, p_2) S_{\Sigma_c^0}(p_1) D_{\Xi_c^0 \Sigma_c^0}(p_1) u(p_1) \quad (15)$$

where $S_{\Sigma_c^0}(p_1) = 1/(m_{\Sigma_c^0} - \not{p}_1)$. The explicit form of D -functions are written down as

$$D_{\Sigma_c^0 \Lambda_c^+ \pi^-} = 12 g_{\Sigma_c^0} g_{\Lambda_c^+} g_{\pi^-} \left[\prod_{i=1}^2 \int \frac{d^4 k_i}{(2\pi)^{4i}} \right] \tilde{\Phi}_{\Sigma_c^0} \left(-\vec{\Omega}_q^2 \right) \tilde{\Phi}_{\Lambda_c^+} \left(-\vec{\Omega}_r^2 \right) \tilde{\Phi}_{\pi^-}(-P^2) \\ \times S_c(k_2) \gamma_\alpha \gamma_5 \text{tr} [\gamma_5 S_u(k_1 + p_2) \gamma_5 S_d(k_1 + p_1) \gamma^\alpha S_d(k_1 + k_2)] \quad (16)$$

where $q_1 = k_2 - w_1^{\text{res}} p_1$, $q_2 = -k_1 - k_2 - w_2^{\text{res}} p_1$, $r_1 = -k_2 + w_1^{\text{out}} p_2$, $r_2 = -k_1 - (1 - w_2^{\text{out}}) p_2$, and $P = k_1 + w_1^M p_1 + w_2^M p_2$. Here the notations are ‘‘res’’ = Σ_c^0 , ‘‘out’’ = Λ_c^+ and $M = \pi^-$.

$$D_{\Xi_c^0 \Sigma_c^0} = 12 g_{\Xi_c^0} g_{\Sigma_c^0} \left[\prod_{i=1}^3 \int \frac{d^4 k_i}{(2\pi)^{4i}} \right] \tilde{\Phi}_{\Xi_c^0} \left(-\vec{\Omega}_q^2 \right) \tilde{\Phi}_{\Sigma_c^0} \left(-\vec{\Omega}_r^2 \right) \\ \times \gamma_\alpha \gamma_5 S_c(k_2 + p_1) O_{\mu L} S_c(k_1 + p_1) \text{tr} [S_d(k_3) \gamma^\alpha S_d(k_3 - k_2) O_L^\mu S_s(k_3 - k_1) \gamma_5] \quad (17)$$

where $q_1 = k_1 + (1 - w_1^{\text{in}}) p_1$, $q_2 = -k_3 - w_2^{\text{in}} p_1$, $r_1 = -k_2 - (1 - w_1^{\text{res}}) p_1$, $r_2 = k_3 + w_2^{\text{res}} p_1$ and ‘‘in’’ = Ξ_c^0 .

By using the mass-shell conditions, one obtains

$$\bar{u}(p_2) D_{\Sigma_c^0 \Lambda_c^+ \pi^-}(p_1, p_2) = \bar{u}(p_2) \gamma_5 (g_{\Sigma_c^0 \Lambda_c^+ \pi^-}^{(0)} + \not{p}_1 g_{\Sigma_c^0 \Lambda_c^+ \pi^-}^{(1)}), \\ D_{\Xi_c^0 \Sigma_c^0}(p_1) u(p_1) = (a_{\Xi_c^0 \Sigma_c^0} + \gamma_5 b_{\Xi_c^0 \Sigma_c^0}) u(p_1). \quad (18)$$

The final expression for the Σ_c^0 -resonance diagram is written as

$$M_{\Sigma_c^0} = \frac{G_F}{\sqrt{2}} \bar{u}(p_2) \left(A_{\Sigma_c^0} + \gamma_5 B_{\Sigma_c^0} \right) u(p_1), \quad (19)$$

where

$$A_{\Sigma_c^0} = V_{\text{CKM}}^{(c)} \left(C_1^{(c)} - C_2^{(c)} \right) \frac{g_{\Sigma_c^0 \Lambda_c^+ \pi^-}^{(-)} b_{\Xi_c^0 \Sigma_c^0}}{m_{\Sigma_c^0} + m_{\Xi_c^0}}, \quad \text{where } g_{\Sigma_c^0 \Lambda_c^+ \pi^-}^{(-)} = g_{\Sigma_c^0 \Lambda_c^+ \pi^-}^{(0)} - m_{\Xi_c^0} g_{\Sigma_c^0 \Lambda_c^+ \pi^-}^{(1)}, \\ B_{\Sigma_c^0} = V_{\text{CKM}}^{(c)} \left(C_1^{(c)} - C_2^{(c)} \right) \frac{g_{\Sigma_c^0 \Lambda_c^+ \pi^-}^{(+)} a_{\Xi_c^0 \Sigma_c^0}}{m_{\Sigma_c^0} - m_{\Xi_c^0}}, \quad \text{where } g_{\Sigma_c^0 \Lambda_c^+ \pi^-}^{(+)} = g_{\Sigma_c^0 \Lambda_c^+ \pi^-}^{(0)} + m_{\Xi_c^0} g_{\Sigma_c^0 \Lambda_c^+ \pi^-}^{(1)}.$$

The matrix elements corresponding to the LD-contributions coming from the second diagram in Fig. 2 with $B_{\text{res}} = \Xi_c^+, \Xi_c'^+$ are calculated in a similar way. We perform the

necessary steps below.

$$M_{\Xi_c^+} = \frac{G_F}{\sqrt{2}} \bar{u}(p_2) \left\{ \left[V_{\text{CKM}}^{(u)} \left(C_1^{(u)} - C_2^{(u)} \right) D_{\Xi_c^+ \Lambda_c^+}^{(u)}(p_2) + V_{\text{CKM}}^{(c)} \left(C_1^{(c)} - C_2^{(c)} \right) D_{\Xi_c^+ \Lambda_c^+}^{(c)}(p_2) \right] \right. \\ \left. \times S_{\Xi_c^+}(p_2) D_{\Xi_c^0 \Xi_c^+ \pi^-}(p_1, p_2) \right\} u(p_1) \quad (20)$$

where

$$D_{\Xi_c^+ \Lambda_c^+}^{(u)}(p_2) = -12 g_{\Xi_c^+} g_{\Lambda_c^+} \left[\prod_{i=1}^3 \int \frac{d^4 k_i}{(2\pi)^{4i}} \right] \tilde{\Phi}_{\Xi_c^+} \left(-\vec{\Omega}_q^2 \right) \tilde{\Phi}_{\Lambda_c^+} \left(-\vec{\Omega}_r^2 \right) \\ \times S_c(k_3) \gamma_\alpha \gamma_5 \text{tr} [S_u(k_2 + p_2) (1 + \gamma_5) S_d(k_2 + k_3) \gamma_5] \\ \times \text{tr} [S_u(k_1 + p_2) \gamma^\alpha S_s(k_1 + k_3) (1 - \gamma_5)] \quad (21)$$

where $q_1 = k_3 - w_1^{\text{res}} p_2$, $q_2 = k_1 + (1 - w_2^{\text{res}}) p_2$, $r_1 = -k_3 + w_1^{\text{out}} p_2$, $r_2 = -k_2 - (1 - w_2^{\text{out}}) p_2$ and “res” = Ξ_c^+ , “out” = Λ_c^+ .

$$D_{\Xi_c^+ \Lambda_c^+}^{(c)}(p_2) = -6 g_{\Xi_c^+} g_{\Lambda_c^+} \left[\prod_{i=1}^3 \int \frac{d^4 k_i}{(2\pi)^{4i}} \right] \tilde{\Phi}_{\Xi_c^+} \left(-\vec{\Omega}_q^2 \right) \tilde{\Phi}_{\Lambda_c^+} \left(-\vec{\Omega}_r^2 \right) \\ \times S_c(k_2 + p_2) O_{\mu L} S_c(k_1 + p_2) \gamma_\alpha \gamma_5 \\ \times \text{tr} [S_u(k_3) \gamma_5 S_d(k_3 - k_2) O_L^\mu S_s(k_3 - k_1) \gamma^\alpha] \quad (22)$$

where $q_1 = k_1 + (1 - w_1^{\text{res}}) p_2$, $q_2 = -k_3 - w_2^{\text{res}} p_2$, $r_1 = -k_2 - (1 - w_1^{\text{out}}) p_2$, $r_2 = k_3 + w_2^{\text{out}} p_2$.

$$D_{\Xi_c^0 \Xi_c^+ \pi^-} = -6 g_{\Xi_c^0} g_{\Xi_c^+} g_{\pi^-} \left[\prod_{i=1}^2 \int \frac{d^4 k_i}{(2\pi)^{4i}} \right] \tilde{\Phi}_{\Xi_c^0} \left(-\vec{\Omega}_q^2 \right) \tilde{\Phi}_{\Xi_c^+} \left(-\vec{\Omega}_r^2 \right) \tilde{\Phi}_{\pi^-} (-P^2) \\ \times \gamma_\alpha \gamma_5 S_c(k_2) \text{tr} [S_u(k_1 + p_2) \gamma_5 S_d(k_1 + p_1) \gamma_5 S_s(k_1 + k_2) \gamma^\alpha] \quad (23)$$

where $q_1 = k_2 - w_1^{\text{in}} p_1$, $q_2 = k_1 + (1 - w_2^{\text{in}}) p_1$, $r_1 = -k_2 + w_1^{\text{res}} p_2$, $r_2 = -k_1 - (1 - w_2^{\text{res}}) p_2$, $P = k_1 + w_1^M p_1 + w_2^M p_2$ and “in” = Ξ_c^0 . By using the mass-shell conditions, one obtains

$$\bar{u}(p_2) D_{\Xi_c^+ \Lambda_c^+}^{(u,c)}(p_2) = \bar{u}(p_2) \left(a_{\Xi_c^+ \Lambda_c^+}^{(u,c)} + \gamma_5 b_{\Xi_c^+ \Lambda_c^+}^{(u,c)} \right) \\ D_{\Xi_c^0 \Xi_c^+ \pi^-}(p_1, p_2) u(p_1) = \gamma_5 \left(g_{\Xi_c^0 \Xi_c^+ \pi^-}^{(0)} + \not{p}_2 g_{\Xi_c^0 \Xi_c^+ \pi^-}^{(1)} \right) u(p_1).$$

The final expression for the second pole diagram is written as

$$M_{\Xi_c^+} = \frac{G_F}{\sqrt{2}} \bar{u}(p_2) \left(A_{\Xi_c^+} + \gamma_5 B_{\Xi_c^+} \right) u(p_1), \quad (24)$$

where

$$A_{\Xi_c^+} = \left\{ V_{\text{CKM}}^{(u)} \left(C_1^{(u)} - C_2^{(u)} \right) b_{\Xi_c^+ \Lambda_c^+}^{(u)} + V_{\text{CKM}}^{(c)} \left(C_1^{(c)} - C_2^{(c)} \right) b_{\Xi_c^+ \Lambda_c^+}^{(c)} \right\} \frac{g_{\Xi_c^0 \Xi_c^+ \pi^-}^{(+)}}{m_{\Xi_c^+} + m_{\Lambda_c^+}}, \\ B_{\Xi_c^+} = \left\{ V_{\text{CKM}}^{(u)} \left(C_1^{(u)} - C_2^{(u)} \right) a_{\Xi_c^+ \Lambda_c^+}^{(u)} + V_{\text{CKM}}^{(c)} \left(C_1^{(c)} - C_2^{(c)} \right) a_{\Xi_c^+ \Lambda_c^+}^{(c)} \right\} \frac{g_{\Xi_c^0 \Xi_c^+ \pi^-}^{(-)}}{m_{\Xi_c^+} - m_{\Lambda_c^+}},$$

where $g_{\Xi_c^0 \Xi_c^+ \pi^-}^{(\pm)} = g_{\Xi_c^0 \Xi_c^+ \pi^-}^{(0)} \pm m_{\Lambda_c^+} g_{\Xi_c^0 \Xi_c^+ \pi^-}^{(1)}$.

$$M_{\Xi_c^+} = \frac{G_F}{\sqrt{2}} \bar{u}(p_2) \left\{ \left[V_{\text{CKM}}^{(u)} \left(C_2^{(u)} - C_1^{(u)} \right) D_{\Xi_c^+ \Lambda_c^+}^{(u)}(p_2) + V_{\text{CKM}}^{(c)} \left(C_2^{(c)} - C_1^{(c)} \right) D_{\Xi_c^+ \Lambda_c^+}^{(c)}(p_2) \right] \right. \\ \left. \times S_{\Xi_c^+}(p_2) D_{\Xi_c^0 \Xi_c^+ \pi^-}(p_1, p_2) \right\} u(p_1) \quad (25)$$

where

$$D_{\Xi_c^+ \Lambda_c^+}^{(u)}(p_2) = 12 g_{\Xi_c^+} g_{\Lambda_c^+} \left[\prod_{i=1}^3 \int \frac{d^4 k_i}{(2\pi)^{4i}} \right] \tilde{\Phi}_{\Xi_c^+} \left(-\vec{\Omega}_q^2 \right) \tilde{\Phi}_{\Lambda_c^+} \left(-\vec{\Omega}_r^2 \right) \\ \times S_c(k_3) \text{tr} [S_u(k_2 + p_2)(1 + \gamma_5) S_d(k_2 + k_3) \gamma_5] \\ \times \text{tr} [S_u(k_1 + p_2) \gamma_5 S_s(k_1 + k_3)(1 - \gamma_5)] \quad (26)$$

where $q_1 = k_3 - w_1^{\text{res}} p_2$, $q_2 = k_1 + (1 - w_2^{\text{res}}) p_2$, $r_1 = -k_3 + w_1^{\text{out}} p_2$, $r_2 = -k_2 - (1 - w_2^{\text{out}}) p_2$ and “res” = Ξ_c^+ , “out” = Λ_c^+ .

$$D_{\Xi_c^+ \Lambda_c^+}^{(c)}(p_2) = -6 g_{\Xi_c^+} g_{\Lambda_c^+} \left[\prod_{i=1}^3 \int \frac{d^4 k_i}{(2\pi)^{4i}} \right] \tilde{\Phi}_{\Xi_c^+} \left(-\vec{\Omega}_q^2 \right) \tilde{\Phi}_{\Lambda_c^+} \left(-\vec{\Omega}_r^2 \right) \\ \times S_c(k_2 + p_2) O_{\mu L} S_c(k_1 + p_2) \\ \times \text{tr} [S_u(k_3) \gamma_5 S_d(k_3 - k_2) O_L^\mu S_s(k_3 - k_1) \gamma_5] \quad (27)$$

where $q_1 = k_1 + (1 - w_1^{\text{res}}) p_2$, $q_2 = -k_3 - w_2^{\text{res}} p_2$, $r_1 = -k_2 - (1 - w_1^{\text{out}}) p_2$, $r_2 = k_3 + w_2^{\text{out}} p_2$.

By using the mass-shell conditions, one obtains

$$\bar{u}(p_2) D_{\Xi_c^+ \Lambda_c^+}^{(u,c)}(p_2) = \bar{u}(p_2) \left(a_{\Xi_c^+ \Lambda_c^+}^{(u,c)} + \gamma_5 b_{\Xi_c^+ \Lambda_c^+}^{(u,c)} \right) \quad (28)$$

It appears that the strong transition $\Xi_c^0 \rightarrow \Xi_c^+ + \pi^-$ is identically equal to zero due to the chosen form of the interpolating quark current as shown in Table I: $\epsilon^{abc} c^a (u^b C \gamma_5 s^c)$. As a result, this transition is described by the diagram which contains the trace of a string with three quark propagators and three γ_5 matrices that gives zero contribution. Explicitly we have

$$D_{\Xi_c^0 \Xi_c^+ \pi^-} = 6 g_{\Xi_c^0} g_{\Xi_c^+} g_{\pi^-} \left[\prod_{i=1}^2 \int \frac{d^4 k_i}{(2\pi)^{4i}} \right] \tilde{\Phi}_{\Xi_c^0} \left(-\vec{\Omega}_q^2 \right) \tilde{\Phi}_{\Xi_c^+} \left(-\vec{\Omega}_r^2 \right) \tilde{\Phi}_{\pi^-} (-P^2) \\ \times S_c(k_2) \text{tr} [S_u(k_1 + p_2) \gamma_5 S_d(k_1 + p_1) \gamma_5 S_s(k_1 + k_2) \gamma_5] \equiv 0. \quad (29)$$

In Ref. [4] it was shown that the vanishing strong coupling for $\Xi_c^0 \rightarrow \Xi_c^+ \pi^-$ transition is a consequence of heavy quark and chiral symmetries. Hence it is a model-independent

statement. Here, one has to comment that there are two kinds of the interpolating currents for the Λ -type baryons (Λ_Q, Ξ_Q) where $Q = b, c$. They are written as $\epsilon^{abc}Q^a(u^b C \gamma_5 s^c)$ (scalar diquark) and $\epsilon^{abc}\gamma_\alpha Q^a(u^b C \gamma^\alpha \gamma_5 s^c)$ (vector diquark). For the details, see Refs [41–44].

It is widely accepted that S-wave amplitude is saturated by the $1/2^-$ resonances, see, e.g., Refs [45, 46] for the original suggestions and [47–50] for the subsequent applications. Ordinarily, their contributions are calculated by using the well-known soft-pion theorem in the current-algebra approach. It allows one to express the parity-violating S-wave amplitude in terms of parity-conserving matrix elements. In our case, one has

$$A_{1/2^-}(\Xi_c^0 \rightarrow \Lambda_c^+ + \pi^-) = \frac{1}{f_\pi} A_{\Xi_c^+ \Lambda_c^+},$$

$$A_{\Xi_c^+ \Lambda_c^+} = V_{\text{CKM}}^{(u)} \left(C_2^{(u)} - C_1^{(u)} \right) a_{\Xi_c^+ \Lambda_c^+}^{(u)} + V_{\text{CKM}}^{(c)} \left(C_2^{(c)} - C_1^{(c)} \right) a_{\Xi_c^+ \Lambda_c^+}^{(c)}. \quad (30)$$

The quantities $a_{\Xi_c^+ \Lambda_c^+}^{(u,c)}$ and $b_{\Xi_c^+ \Lambda_c^+}^{(u,c)}$ are defined by Eqs. (26)-(28).

Finally, the transition $\Xi_c^0 \rightarrow \Lambda_c^+ + \pi^-$ amplitude is written in terms of invariant amplitudes as

$$\langle \Lambda_c^+ \pi^- | \mathcal{H}_{\text{eff}} | \Xi_c^0 \rangle = \frac{G_F}{\sqrt{2}} \bar{u}(p_2) (A + \gamma_5 B) u(p_1) \quad (31)$$

where A and B are given by

$$A = A_{\text{SD}} + A_{\text{LD}}, \quad A_{\text{LD}} = A_{\Sigma_c^0} + A_{\Xi_c'^+} + A_{1/2^-},$$

$$B = B_{\text{SD}} + B_{\text{LD}}, \quad B_{\text{LD}} = B_{\Sigma_c^0} + B_{\Xi_c'^+}. \quad (32)$$

It is more convenient to use helicity amplitudes $H_{\lambda_1 \lambda_M}$ instead of invariant ones A and B as described in [51]. One has

$$H_{\frac{1}{2}t}^V = \sqrt{Q_+} A, \quad H_{\frac{1}{2}t}^A = \sqrt{Q_-} B, \quad (33)$$

where $m_\pm = m_1 \pm m_2$, $Q_\pm = m_\pm^2 - q^2$.

Finally, the two-body decay width reads

$$\Gamma(B_1 \rightarrow B_2 + M) = \frac{G_F^2 |\mathbf{p}_2|}{32\pi m_1^2} \mathcal{H}_S, \quad \mathcal{H}_S = 2 \left(\left| H_{\frac{1}{2}t}^V \right|^2 + \left| H_{\frac{1}{2}t}^A \right|^2 \right) \quad (34)$$

where $|\mathbf{p}_2| = \lambda^{1/2}(m_1^2, m_2^2, q^2)/(2m_1)$.

IV. NUMERICAL RESULTS

Our covariant constituent quark model contains a number of model parameters which have been determined by a global fit to a multitude of decay processes. The values of the

constituent quark masses m_q are taken from the last fit in [17]. In the fit, the infrared cutoff parameter λ of the model has been kept fixed as found in the original paper [14]. Table II shows as below: The size parameters of light meson were fixed by fitting the data on the leptonic decay constant. The numerical values of the size parameters and the leptonic decay constants for pion is shown in Table III.

TABLE II: Constituent quark masses and infrared cutoff parameter λ .

$m_{u/d}$	m_s	m_c	λ	
0.241	0.428	2.16	0.181	GeV

TABLE III: Size parameter and leptonic decay constant of pion.

Meson	Λ_M (GeV)	f_M (MeV)	f_M^{expt} (MeV)
Pion	0.871	130.3	130.41 ± 0.20

Since the experimental data of the single charm baryon decays become to appear recently, we will assume for the time being that the size parameters of all single charm baryons are the same. In Fig. 5 we plot the dependence on this parameter denoted as Λ_c of branching fractions $\Xi_c^0 \rightarrow \Lambda_c^+ + \pi^-$. One can see that the measured branching fraction can be accommodated in the framework of this work by having $\Lambda_c \approx 0.61$ GeV. In addition to the line describing the central value of the experimental data, we also display the strip corresponding to experimental uncertainties. In order to estimate the uncertainty caused by the choice of the size parameter we allow the size parameter to vary from $\Lambda_{c\text{min}} = 0.54$ to $\Lambda_{c\text{max}} = 0.66$ GeV that correspond to the intersections of the theoretical curve for branching fraction with the experimental lower and upper error bars.

We evaluate the mean $\bar{\Gamma} = \sum_{i=1}^N \Gamma_i / N$ and the mean square deviation $\sigma^2 = \sum_{i=1}^N (\Gamma_i - \bar{\Gamma})^2 / N$. Finally, our result for the branching fraction reads as

$$\mathcal{B}(\Xi_c^0 \rightarrow \Lambda_c^+ + \pi^-) = (0.54 \pm 0.11)\% \quad (35)$$

which should be compared with the data from LHCb and Belle: $\mathcal{B} = (0.55 \pm 0.02 \pm 0.18)\%$ [1] and $\mathcal{B} = (0.54 \pm 0.05 \pm 0.12)\%$ [2].

For comparison, we plot in Fig. 5 both the separate SD-contributions coming from the diagrams with topologies Ia, IIa, IIb, and III and the LD-contributions coming from the pole diagrams. It is readily seen that the SD-contributions are much smaller than those coming from the pole LD-diagrams.

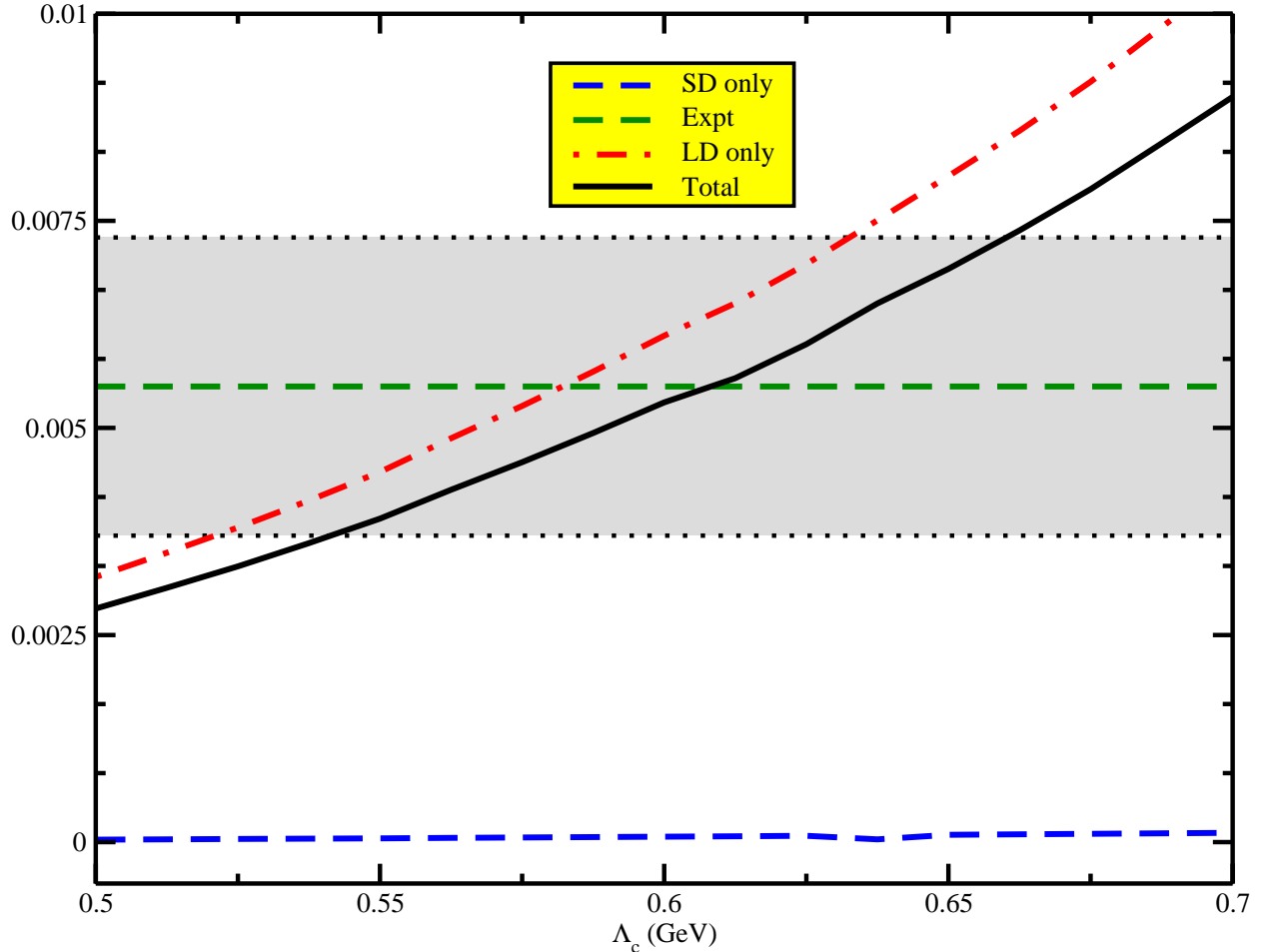


FIG. 5: Dependence of the branching fractions on the size parameter.

The numerical results for the SD, LD and full amplitudes are shown in Table IV. One can see that $|A_{LD}| > |A_{SD}|$.

TABLE IV: SD, LD and full amplitudes in units of GeV^2 .

Amplitudes	SD	LD	SD+LD
A-ampl.	0.0156	-0.0751	-0.0595
B-ampl.	0.166	-5.378	-5.212

Also it would be instructive to evaluate the asymmetry parameter defined by

$$\alpha = \frac{|H_{1/2t}|^2 - |H_{-1/2t}|^2}{|H_{1/2t}|^2 + |H_{-1/2t}|^2} = -\frac{2\kappa AB}{A^2 + \kappa^2 B^2}, \quad (36)$$

where $\kappa = |\mathbf{p}_2|/(E_2 + m_2)$ and $E_2 = (m_1^2 + m_2^2 - q^2)/(2m_1)$. The numerical value of the asymmetry parameter is found to be equal to

$$\alpha = -0.751. \quad (37)$$

Finally, we compare our results obtained for the branching fraction and the asymmetry parameter with other the data and other approaches in Table V.

TABLE V: Comparison of our findings with other approaches.

Approach	BR($\Xi_c^0 \rightarrow \Lambda_c^+ \pi^-$)%	Asymmetry
Our model	0.54 ± 0.11	-0.75
LHCb [1]	$0.55 \pm 0.02 \pm 0.1$...
Belle [2]	$0.54 \pm 0.05 \pm 0.12$...
Voloshin [6]	$> 0.025 \pm 0.015$...
Gronau and Rosner [8] (construc)	0.194 ± 0.070	...
Gronau and Rosner [8] (destruc)	< 0.01	...
Faller and Mannel [9]	< 0.39	...
Cheng et al. [12]	0.72 ± 0.07	0.46 ± 0.05
Niu et al. [13]	0.58 ± 0.21	-0.16

V. SUMMARY AND CONCLUSION

We have studied two-body nonleptonic $\Delta C = 0$ decay $\Xi_c^0 \rightarrow \Lambda_c^+ + \pi^-$ in the framework of the covariant confined quark model (CCQM) with account for both short and long distance effects. The short distance effects are induced by four topologies of external and internal weak W -interactions, while long distance effects are saturated by an inclusion of the so-called

pole diagrams. Pole diagrams are generated by resonance contributions of the low-lying spin $\frac{1}{2}^+$ (Σ_c^0 and $\Xi_c'^+$) and spin $\frac{1}{2}^-$ baryons. The last contributions are calculated by using the well-known soft-pion theorem. It is found that the contribution of the SD diagrams is significantly suppressed, by more than one order of magnitude in comparison with data. The most significant contributions are coming from the intermediate $\frac{1}{2}^+$ and $\frac{1}{2}^-$ resonances. We can get consistency with the experimental data for the value of size parameter being equal to $\Lambda \approx 0.61$ GeV.

Acknowledgments

The research has been funded by the Science Committee of the Ministry of Science and Higher Education of the Republic of Kazakhstan (Grant No. AP19678771). V.E.L. acknowledges the support by ANID PIA/APOYO AFB220004 (Chile), by FONDECYT (Chile) under Grant No. 1230160, and by ANID–Millennium Program–ICN2019_044 (Chile).

-
- [1] R. Aaij *et al.* [LHCb], Phys. Rev. D **102**, no.7, 071101 (2020) [arXiv:2007.12096 [hep-ex]].
- [2] S. S. Tang *et al.* [Belle], Phys. Rev. D **107**, no.3, 032005 (2023) [arXiv:2206.08527 [hep-ex]].
- [3] S. Groote and J. G. Körner, Eur. Phys. J. C **82**, no.4, 297 (2022) [arXiv:2112.14599 [hep-ph]].
- [4] H. Y. Cheng, C. Y. Cheung, G. L. Lin, Y. C. Lin, T. M. Yan and H. L. Yu, Phys. Rev. D **46**, 5060-5068 (1992)
- [5] M. B. Voloshin, Phys. Lett. B **476**, 297-302 (2000) [arXiv:hep-ph/0001057 [hep-ph]].
- [6] M. B. Voloshin, Phys. Rev. D **100**, no.11, 114030 (2019) [arXiv:1911.05730 [hep-ph]].
- [7] R. Aaij *et al.* [LHCb], Phys. Rev. D **100**, no.3, 032001 (2019) [arXiv:1906.08350 [hep-ex]].
- [8] M. Gronau and J. L. Rosner, Phys. Lett. B **757**, 330-333 (2016) [arXiv:1603.07309 [hep-ph]].
- [9] S. Faller and T. Mannel, Phys. Lett. B **750**, 653-659 (2015) [arXiv:1503.06088 [hep-ph]].
- [10] H. Y. Cheng, C. Y. Cheung, G. L. Lin, Y. C. Lin, T. M. Yan and H. L. Yu, JHEP **03**, 028 (2016) [arXiv:1512.01276 [hep-ph]].
- [11] H. Y. Cheng and F. Xu, Phys. Rev. D **105**, no.9, 094011 (2022) [arXiv:2204.03149 [hep-ph]].
- [12] H. Y. Cheng, C. W. Liu and F. Xu, Phys. Rev. D **106**, no.9, 093005 (2022) [arXiv:2209.00257 [hep-ph]].
- [13] P. Y. Niu, Q. Wang and Q. Zhao, Phys. Lett. B **826**, 136916 (2022) [arXiv:2111.14111 [hep-ph]].
- [14] T. Branz, A. Faessler, T. Gutsche, M. A. Ivanov, J. G. Körner and V. E. Lyubovitskij, Phys. Rev. D **81**, 034010 (2010) [arXiv:0912.3710 [hep-ph]].
- [15] T. Gutsche, M. A. Ivanov, J. G. Körner, V. E. Lyubovitskij and Z. Tyulemissov, Phys. Rev. D **99**, no.5, 056013 (2019) [arXiv:1812.09212 [hep-ph]].
- [16] M. A. Ivanov, J. G. Körner, V. E. Lyubovitskij and Z. Tyulemissov, Phys. Rev. D **104**, no.7, 074004 (2021) [arXiv:2107.08831 [hep-ph]].
- [17] T. Gutsche, M. A. Ivanov, J. G. Körner, V. E. Lyubovitskij, P. Santorelli and N. Habył, Phys. Rev. D **91**, no.7, 074001 (2015) [erratum: Phys. Rev. D **91**, no.11, 119907 (2015)] [arXiv:1502.04864 [hep-ph]].
- [18] M. A. Ivanov, J. G. Körner and V. E. Lyubovitskij, Phys. Part. Nucl. **51**, no.4, 678-685 (2020)
- [19] M. A. Ivanov, Particles **3**, no.1, 123-144 (2020)
- [20] T. Gutsche, M. A. Ivanov, J. G. Körner, V. E. Lyubovitskij and Z. Tyulemissov, Phys. Rev.

- D **100**, no.11, 114037 (2019) [arXiv:1911.10785 [hep-ph]].
- [21] T. Gutsche, M. A. Ivanov, J. G. Körner and V. E. Lyubovitskij, *Particles* **2**, no.2, 339-356 (2019)
- [22] T. Gutsche, M. A. Ivanov, J. G. Körner and V. E. Lyubovitskij, *Phys. Rev. D* **98**, no.7, 074011 (2018) [arXiv:1806.11549 [hep-ph]].
- [23] M. A. Ivanov, *PoS EPS-HEP2017*, 220 (2017) [arXiv:1711.10821 [hep-ph]].
- [24] T. Gutsche, M. A. Ivanov, J. G. Körner and V. E. Lyubovitskij, *Phys. Rev. D* **96**, no.5, 054013 (2017) [arXiv:1708.00703 [hep-ph]].
- [25] T. Gutsche, M. A. Ivanov, J. G. Körner, V. E. Lyubovitskij, V. V. Lyubushkin and P. Santorelli, *Phys. Rev. D* **96**, no.1, 013003 (2017) [arXiv:1705.07299 [hep-ph]].
- [26] T. Gutsche, M. A. Ivanov, J. G. Körner, V. E. Lyubovitskij and P. Santorelli, *Phys. Rev. D* **93**, no.3, 034008 (2016) [arXiv:1512.02168 [hep-ph]].
- [27] T. Gutsche, M. A. Ivanov, J. G. Körner, V. E. Lyubovitskij and P. Santorelli, *Phys. Rev. D* **92**, no.11, 114008 (2015) [arXiv:1510.02266 [hep-ph]].
- [28] N. Habyl, T. Gutsche, M. A. Ivanov, J. G. Körner, V. E. Lyubovitskij and P. Santorelli, *Int. J. Mod. Phys. Conf. Ser.* **39**, 1560112 (2015) [arXiv:1509.07688 [hep-ph]].
- [29] T. Gutsche, M. A. Ivanov, J. G. Körner, V. E. Lyubovitskij and P. Santorelli, *Phys. Rev. D* **90**, no.11, 114033 (2014) [erratum: *Phys. Rev. D* **94**, no.5, 059902 (2016)] [arXiv:1410.6043 [hep-ph]].
- [30] T. Gutsche, M. A. Ivanov, J. G. Körner, V. E. Lyubovitskij and P. Santorelli, *Phys. Rev. D* **88**, no.11, 114018 (2013) [arXiv:1309.7879 [hep-ph]].
- [31] T. Gutsche, M. A. Ivanov, J. G. Körner, V. E. Lyubovitskij and P. Santorelli, *Phys. Rev. D* **87**, 074031 (2013) [arXiv:1301.3737 [hep-ph]].
- [32] T. Gutsche, M. A. Ivanov, J. G. Körner, V. E. Lyubovitskij and P. Santorelli, *Phys. Rev. D* **86**, 074013 (2012) [arXiv:1207.7052 [hep-ph]].
- [33] A. De Rujula, H. Georgi and S. L. Glashow, *Phys. Rev. D* **12**, 147-162 (1975)
- [34] J. G. Körner, M. Kramer and D. Pirjol, *Prog. Part. Nucl. Phys.* **33**, 787-868 (1994) [arXiv:hep-ph/9406359 [hep-ph]].
- [35] R. L. Workman *et al.* [Particle Data Group], *PTEP* **2022**, 083C01 (2022)
- [36] G. Buchalla, A. J. Buras and M. E. Lautenbacher, *Rev. Mod. Phys.* **68**, 1125-1144 (1996) [arXiv:hep-ph/9512380 [hep-ph]].

- [37] A. Salam, *Nuovo Cimento* **25**, 224 (1962).
- [38] S. Weinberg, *Phys. Rev.* **130**, 776 (1963).
- [39] K. Hayashi, M. Hirayama, T. Muta, N. Seto, and T. Shirafuji, *Fortsch. Phys.* **15**, 625 (1967).
- [40] G. V. Efimov and M. A. Ivanov, *The Quark Confinement Model of Hadrons*, (IOP Publishing, Bristol & Philadelphia, 1993)
- [41] E. V. Shuryak, *Nucl. Phys. B* **198**, 83-101 (1982)
- [42] A. G. Grozin and O. I. Yakovlev, *Phys. Lett. B* **285**, 254-262 (1992) [arXiv:hep-ph/9908364 [hep-ph]].
- [43] S. Groote, J. G. Körner and O. I. Yakovlev, *Phys. Rev. D* **54**, 3447-3456 (1996) [arXiv:hep-ph/9604349 [hep-ph]].
- [44] M. A. Ivanov, V. E. Lyubovitskij, J. G. Körner and P. Kroll, *Phys. Rev. D* **56**, 348-364 (1997) [arXiv:hep-ph/9612463 [hep-ph]].
- [45] R. E. Marshak, Riazuddin, and C. P. Ryan, *Theory of weak interactions in particle physics*, New York, Wiley-Interscience, 1969, 761 p.
- [46] D. Bailin, *Weak Interactions*, Sussex University Press, Chatto & Windus, 1977, 406 p.
- [47] D. Ebert and W. Kallies, *Yad. Fiz.* **40**, 1250 (1984) [*Sov. J. Nucl. Phys.* **40**, 794 (1984)].
- [48] D. Ebert and W. Kallies, *Phys. Lett. B* **131**, 183 (1983), *B* **148**, 502(E) (1984)
- [49] H. Y. Cheng, *Z. Phys. C* **29**, 453 (1985)
- [50] H. Y. Cheng, X. W. Kang, and F. Xu, *Phys. Rev. D* **97**, 074028 (2018) [arXiv:1801.08625 [hep-ph]].
- [51] J. G. Körner and M. Krämer, *Z. Phys. C* **55**, 659 (1992).